

ARCHIVE COPY

DOC NOM SER CN
UNC22512-PDC A 1



**EFFECTS OF CONDENSATION ON
GAS VELOCITY IN
A FREE-JET EXPANSION**

A. B. Bailey

ARO, Inc.

June 1973

Approved for public release; distribution unlimited.

**VON KÁRMÁN GAS DYNAMICS FACILITY
ARNOLD ENGINEERING DEVELOPMENT CENTER
AIR FORCE SYSTEMS COMMAND
ARNOLD AIR FORCE STATION, TENNESSEE**

Property of U. S. Air Force
AEDC LIBRARY
F40600-73-C-0004



AEDC TECHNICAL LIBRARY



5 0720 00033 5697

NOTICES

When U. S. Government drawings specifications, or other data are used for any purpose other than a definitely related Government procurement operation, the Government thereby incurs no responsibility nor any obligation whatsoever, and the fact that the Government may have formulated, furnished, or in any way supplied the said drawings, specifications, or other data, is not to be regarded by implication or otherwise, or in any manner licensing the holder or any other person or corporation, or conveying any rights or permission to manufacture, use, or sell any patented invention that may in any way be related thereto.

Qualified users may obtain copies of this report from the Defense Documentation Center.

References to named commercial products in this report are not to be considered in any sense as an endorsement of the product by the United States Air Force or the Government.

EFFECTS OF CONDENSATION ON
GAS VELOCITY IN
A FREE-JET EXPANSION

A. B. Bailey
ARO, Inc.

Approved for public release; distribution unlimited.

FOREWORD

The research reported herein was conducted by the Arnold Engineering Development Center (AEDC) under sponsorship of Air Force Cambridge Research Laboratories (AFCRL), Air Force Systems Command (AFSC), under Program Element 62101F.

The results presented herein were obtained by ARO, Inc. (a subsidiary of Sverdrup & Parcel and Associates, Inc.), contract operator of AEDC, AFSC, Arnold Air Force Station, Tennessee. This work was conducted from April 1970 to July 1972 under ARO Project Nos. VW5140 and VW5224. The manuscript was submitted for publication on April 13, 1973.

This technical report has been reviewed and is approved.

EULES L. HIVELY
Research & Development Division
Directorate of Technology

ROBERT O. DIETZ
Director of Technology

ABSTRACT

An aerodynamic molecular beam has been used in an attempt to develop criteria for the determination of the onset of condensation in free-jet expansions of various gases. Measurements have been made of the total and monomer velocity distribution as a function of source pressure for the following conditions: (1) sonic orifice diameters of 0.0147, 0.0386, and 0.1245 cm, (2) source temperatures from 85 to 450°K, (3) source pressures from 10 to 10,000 torr, (4) argon, nitrogen, oxygen, carbon monoxide, and carbon dioxide test gases, and (5) 20°K skimmer and collimator surfaces. The variation of beam velocity with source pressure was characterized by an approximately constant value up to a particular pressure at which point the velocity started to increase. For all the gases tested it was found that, for each orifice size, $p/T^{2.5}$ is constant at the point of velocity increase. The variation of this constant with orifice diameter is a function of the test gas. The velocity increase results from the addition of the heat of vaporization to the gas. From a knowledge of the velocity increase and the properties of the gas, estimates of the fraction of condensate have been made. These estimates indicate a mass fraction of condensate ranging from approximately 20 to 30 percent. There are indications from some of the velocity measurements that contributions from evaporated or sublimated molecules may be affecting some of the velocity distributions. This is of particular importance in sampling from condensed flows, and further studies are required to determine the degree of evaporation.

CONTENTS

	<u>Page</u>
ABSTRACT	iii
NOMENCLATURE	vi
I. INTRODUCTION	1
II. APPARATUS	
2.1 Aerodynamic Molecular Beam System	1
2.2 Beam Source	1
2.3 Detector Systems	2
III. EXPERIMENTAL PROCEDURES	4
IV. RESULTS AND DISCUSSION	
4.1 Indicators of Condensation in a Free-Jet Expansion	5
4.2 Beam Velocity Distribution as a Function of Source Pressure	7
4.3 Effect of Source Diameter, Pressure, and Temperature on Beam Mean Velocity	8
4.4 Estimates of Mass Fraction of Condensate from Gas Velocity Measurements	9
4.5 Acceleration of Clusters in Free-Jet Expansions	10
V. CONCLUSIONS	12
REFERENCES	13

APPENDIXES

I. ILLUSTRATIONS

Figure

1. Schematic of the Aerodynamic Molecular Beam Chamber	17
2. Schematic of the Temperature-Controlled Molecular Beam Source	18
3. Schematic Diagram of the Modulated Beam Detection System Used in Relative Cluster Abundance Measurements	19

<u>Figure</u>	<u>Page</u>
4. Schematic Diagram of the Modulated Beam Detection System Used in the Time-of-Flight Measurements . . .	20
5. Indicators of Condensation in Free-Jet Expansions . . .	21
6. Effect of Source Pressure on Monomer Velocity Distribution for Nitrogen	23
7. Mean Beam Velocity as a Function of Source Pressure	24
8. Source Pressure at Which Gas Velocity Increases as a Function of Source Temperature	26
9. Source Pressure at Which Gas Velocity Increases as a Function of Source Diameter	27
10. Effect of Source-to-Skimmer Distance on Measured Total Beam Velocity in Condensed Flow of Carbon Dioxide	28

II. TABLE

I. Mass Fraction of Condensate Derived from Measurements of Beam Velocity	29
---	----

NOMENCLATURE

C_p	Constant pressure specific heat
d	Orifice diameter
g	Mass fraction of condensate
h_o	Source stagnation enthalpy
h_∞	Free-stream static enthalpy
L	Latent heat of vaporization
p_o	Source stagnation pressure
T_o	Source stagnation temperature
$(V_\infty)_{nc}$	Gas velocity with no condensation
$(V_\infty)_c$	Gas velocity with condensation

SECTION I INTRODUCTION

For several years, experimental investigation of condensation phenomena in free-jet expansions has been conducted in the Aerodynamic Molecular Beam Chamber at the Arnold Engineering Development Center (AEDC). It has been observed that when a jet expands into a high-vacuum environment, condensation can occur, resulting in the formation of molecular clusters which lead to changes in flow properties. A detailed discussion and summary of previous experimental work is contained in Ref. 1. In that report measurements of total, monomer, dimer, trimer, etc. beam intensities and velocity distributions are presented for a range of orifice diameters, source temperatures and pressures, test gases, and beam-geometry configurations. The present report deals with one facet of condensation phenomena, namely the effect of condensation on the mean gas velocity.

SECTION II APPARATUS

2.1 AERODYNAMIC MOLECULAR BEAM SYSTEM

The AEDC Aerodynamic Molecular Beam Chamber (Fig. 1, Appendix I) is a 3-1/2-ft-diam, 6-1/2-ft-long stainless steel chamber divided into two sections by a removable bulkhead. Vacuum conditions are produced by oil diffusion pumps and 77°K liquid nitrogen- and 20°K gaseous helium-cooled cryoliners. This pumping system produces base pressures of 10^{-8} torr and maintains pressures of 1×10^{-6} and 1×10^{-7} torr in the source and test chambers, respectively, during testing.

The molecular beam was produced from the free-jet expansion of the test gas from an aerodynamic molecular beam source (Section 2.2). The jet was sampled by skimming a stream tube from the flow using a 1.27-cm 20°K stainless steel skimmer and a 0.4-cm 20°K stainless steel collimator (Fig. 1).

2.2 BEAM SOURCE

A schematic of the molecular beam source is shown in Fig. 2. The test gas flows through the center tube, which vents into a settling

chamber prior to passing through the test orifice. The heating (or cooling) fluid passes through two tubes concentric with the gas supply tube. The source is approximately 4 ft long; this length, together with that of the settling chamber, should give the test gas sufficient time to accommodate to the temperature of the circulating fluid. The temperature of the test gas is measured with a copper-constantan thermocouple located at the upstream end of the settling chamber. Temperatures in the range from 80 to 430°K are achieved as follows:

1. For 80 to 170°K, liquid nitrogen is circulated through the source.
2. For 180 to 250°K, liquid nitrogen is circulated through a reservoir containing Freon MF[®]. The nitrogen flow rate is adjusted so that the desired temperature is achieved in the Freon, which is then pumped through the source.
3. For 280 to 300°K, water is pumped through the source.
4. For 350 to 430°K, gaseous nitrogen is passed through a resistance-heated stainless steel tube and then through the source.

A thin-wall stainless steel bellows (Fig. 1) permits the source to be moved in the vertical and horizontal planes. It is adjusted until the beam intensity as measured by the miniature General Electric (GE) ionization gage is at maximum. At this point it is assumed that the source is correctly aligned with the skimmer and collimator.

The orifices were made in 0.005-cm stainless steel shim stock silver-soldered to the orifice insert (Fig. 2): Various diameter orifices were then cut into the stainless steel using an Elox[®] process. Examination of these orifices showed that they were not smooth and circular, and a honing and polishing procedure was instituted which corrected this problem. The three orifices used in the present series of tests had diameters of 0.0147, 0.0386, and 0.1245 cm.

2.3 DETECTOR SYSTEMS

The test section of the chamber contains the molecular beam detection apparatus. The detector systems which are discussed allow the measurement of total beam intensities, individual mass specie intensities, and individual mass specie velocity distributions.

2.3.1 Total Beam Intensity Detector System

The total beam intensity was measured with a miniature ionization gage positioned on the beam centerline. For these measurements the normal 2.54-cm-diam opening of the gage was reduced to 0.6 cm. This reduction in opening served to (1) increase the sensitivity of the gage to directed gas flows and (2) ensure that molecular clusters were broken up by wall collisions and that a gage response was obtained before the molecules escaped.

2.3.2 Modulated Beam Detector

The modulated beam detection system consists of (1) a mechanical beam chopper, (2) a quadrupole mass spectrometer (2 to 600 amu), and (3) a lock-in (narrow bandpass) amplifier. A schematic of the system is shown in Fig. 3, and a detailed description is given in Ref. 2.

The collimated molecular beam is chopped into pulses by a slotted rotating wheel. The wheel is driven by a small two-phase vacuum-rated synchronous motor at approximately 75 Hz. A photo-etching technique was used to make 20 equally spaced 1.9- by 0.16-cm slots in a 0.005-cm-thick stainless steel wheel. The beam to be chopped by the wheel is defined by a 0.16- by 0.16-cm orifice in a 0.005-cm-thick stainless steel plate located upstream of the wheel. After the beam has been chopped, the pulsed gas passes through the ionization region of the mass spectrometer. An ionized sample of the beam is deflected into the quadrupole section, which is tuned to a particular mass number. The resulting ion current is amplified by an electron multiplier, which sends a pulsed signal to the lock-in amplifier. A light and a photocell detector, mounted at the chopper wheel, provide the chopping frequency to the amplifier and keep it synchronized with the actual molecular beam modulation frequency. The lock-in amplifier increases the signal-to-noise ratio by amplifying only those signals having the proper frequency and phase with respect to the reference signal from the photocell. This amplified signal, recorded on a voltmeter, is a measure of the intensity of the mass number under investigation.

2.3.3 Velocity Distribution Detection System

A detailed description of this system is contained in Ref. 3, and its components are shown schematically in Fig. 4. After the collimated beam passes through the chopper wheel, the molecules spread according to their velocity distribution. The beam then passes through the ionizing

section of the mass spectrometer. The spectrometer operates as a flow density detector and measures the local particle density as a function of time.

The quadrupole section is tuned to the mass number of interest, and the resulting ion current is amplified by an electron multiplier. A time reference for the spectrometer output is provided by the light and photocell arrangement shown in Fig. 4. The mass spectrometer signal represents the molecular arrival rate, which is time dependent, referenced to a particular "start time" plus the random noise of the background gas. (The "start time" is the time the chopper shutter opens.) The signal is then processed in a waveform eductor, which is basically a device for extracting a weak signal from a high-noise background. In the present application, the resulting output from the waveform eductor is recorded by photographing the oscilloscope trace. The trace represents the time-of-flight (TOF) of beam molecules, from which the velocity distribution may be inferred.

SECTION III EXPERIMENTAL PROCEDURES

Basically, three sets of measurements were made, as follows:

1. beam intensities of monomer, dimer, trimer, etc. cluster ions
2. total beam intensity
3. incident beam TOF distributions.

These measurements were made at the following test conditions:

(1) source pressures varying from 5 to 10,000 torr, (2) source temperatures ranging from 85 to 450°K, (3) sonic orifice diameters of 0.0147, 0.0386, and 0.1245 cm, and (4) argon, nitrogen, oxygen, carbon monoxide, and carbon dioxide test gases.

The nondimensionalized source-to-skimmer distances for the 0.0147-, 0.0386-, and 0.1245-cm-diam sources were approximately 1500, 590, and 630 source diameters, respectively. The rationale for the present investigation was not to establish the optimum nozzle skimmer separation distance for each orifice but rather to vary the pressure, temperature, and source gas at a fixed source-to-skimmer distance.

Individual mass beam intensity measurements were obtained with the modulated beam detection system. In measurements of this type the mass spectrometer was tuned to the mass number of interest, and the output voltage was monitored as the source pressure was incrementally increased. All external spectrometer settings were held constant during these tests. Normally, the extraction, focus, and ion energy voltages are held constant at 10, 135, and 22v, respectively, and the emission current and electron energy are held at 0.2 ma and 90 v, respectively. The electron multiplier voltage was varied from 1500 to 3000 v, depending on the magnitude of the signal.

For measurements of incident beam velocity, the mass spectrometer was tuned to the mass number of interest, and the signal was then correctly phased. In this study the velocity of interest was that which occurred at the time of maximum output signal which, for high-speed ratios, is essentially equal to the mean velocity of the gas (Ref. 4). To calculate this velocity, it is necessary to know (1) the flight distance and (2) the total flight time. Throughout the present series of tests the flight distance varied from 25.75 to 53 cm. The total TOF is comprised of a consideration of (1) the shutter opening time, which can be calculated from a knowledge of the chopper diameter and the slot width, (2) the time between the photocell output and the output of the first waveform eductor module (this time interval was measured to an accuracy of 1 μ sec with a 10-MHz Beckman counter), (3) the total sweep time of the waveform eductor, also measured to an accuracy of 1 μ sec with a Beckman counter, and (4) the flight time in the mass spectrometer itself (this has been derived for various mass numbers in earlier experiments (e.g., Ref. 1)).

SECTION IV RESULTS AND DISCUSSION

4.1 INDICATORS OF CONDENSATION IN A FREE-JET EXPANSION

With the onset of condensation in a free-jet expansion, the following processes would be expected to occur as the source pressure is increased: (1) formation of molecular clusters, dimers, trimers, etc.; (2) appearance of liquid droplets; and (3) formation of crystals. The source pressures at which these phase changes occur in an argon beam have been identified using an electron diffraction technique (Ref. 5) and

are shown in Fig. 5a. Also shown in Fig. 5a for similar beam source conditions are measurements of (1) total monomer, dimer, trimer, and tetramer beam intensity and monomer velocity obtained in the present study; and (2) characteristic cluster size (Ref. 6). The present results (Fig. 5a) indicate that the monomer and total beam intensity diverge and the monomer velocity increases at a source pressure where Audit's data (Ref. 5) show a change from an all-monomer flow to one containing molecular clusters and liquid droplets. Audit (Ref. 5) was unable to estimate the size of the clusters he observed. A more recent electron diffraction analysis (Ref. 7) has shown that in an argon expansion from a source pressure of 900 torr the mean cluster size is about 20 atoms/cluster. The nucleation of nitrogen has been studied using crossed beam and accelerating potential techniques (Ref. 8). The results of these analyses, which are shown in Fig. 5b, indicate that clusters ranging in size from 10^2 to 10^4 molecules can exist for stagnation pressures varying from 50 to 10^4 torr. If it is assumed that both these analyses, i. e., Refs. 7 and 8, give a reasonably accurate measure of the cluster size, then clusters comprised of at least 20 molecules (or atoms) are shown to exist at source pressures where (1) the gas velocity increases and (2) the monomer and total beam intensities first deviate. This lends support to the suggestion made earlier (Ref. 1) that these beam characteristics are indicative of condensation onset.

The main effects of condensation on the flow as a whole are (1) a depletion of the monomers and (2) heating of the remaining gas as a result of the addition of the latent heat of vaporization to the flow. Thus, the effects of condensation are similar to those of heat addition, which in supersonic flow results in an increase in stream temperature and pressure. Increases in temperature are reflected in increases in (1) monomer velocity (Figs. 5a and b) and (2) monomer free-stream static temperature (c.f., Fig. 39, Ref. 1). Sherman (Ref. 9) has shown that when condensation occurs in an expanding flow the gas enthalpy increase is directly proportional to the product of the latent heat of vaporization and the mass fraction of the condensate. With the present velocity-measuring system the effects of condensation on monomer beam velocity will become detectable only when there is a sufficiently large number of clusters to affect the mean-flow properties of the remaining gas. The reported observation (Ref. 8) of a 100-molecule cluster in the nitrogen expansion (Fig. 5b) without any detectable increase in mean gas velocity suggests that the number density of these clusters may be small at this source pressure.

4.2 BEAM VELOCITY DISTRIBUTION AS A FUNCTION OF SOURCE PRESSURE

A series of velocity distributions obtained with the mass spectrometer operating in the side-on mode is presented in Fig. 6. As noted earlier (Section III), the velocity of interest in the present study is that occurring at the time of maximum signal which, for high-speed ratios, is approximately equal to the mean velocity of the gas (Ref. 4). This velocity, V , is defined as

$$V = \frac{L}{t}$$

where L is the flight distance and t is the time to maximum signal.

The velocity distributions shown in Fig. 6 fall into the three following categories: (1) $p_0 \lesssim 80$ torr, where the time to maximum signal is constant, indicating a constant monomer velocity. The width of the ion current distribution at half maximum signal decreases with increasing source pressure, indicating a decreasing free-stream static temperature; (2) $150 \lesssim p_0 \lesssim 2000$ torr, where the velocity distributions indicate an increasing monomer velocity and continued decrease in free-stream static temperature; (3) $p_0 \gtrsim 4000$, where the form of the ion current distribution changes. The time to maximum signal increases (indicating a decrease in monomer gas velocity), and the width of the distribution at half the maximum signal increases.

The nature of these changes is characterized by the ion current distribution obtained for $p_0 = 6000$ torr (see Fig. 6). The observed asymmetry of this distribution arises from an increase in the number of slower-moving monomer ions. It is postulated that these slower-moving monomers are a result of fragmentation of the slower-moving large clusters by electron impact in the ionization region of the mass spectrometer. The contribution of these slower-moving fragmentation monomers to the total monomer ion current is not large enough to produce a detectable asymmetry in the ion current distributions for $p_0 \lesssim 100$ torr. With increasing source pressure the number of slower-moving monomers increases with respect to those that have been accelerated, resulting in a decrease in the mean monomer velocity. The possible explanation for the symmetrical ion current distribution for $p_0 = 8000$ torr is that at this source pressure the contributions from the fast and slow molecules are approximately equal.

If the above explanation is correct, then for $p_0 > 1000$ torr the monomer and dimer intensity measurements shown in Fig. 5b contain a significant contribution from the fragmentation of the large clusters in the ionization region of the mass spectrometer. Thus, caution should be exercised in any attempts to determine the chemical kinetics of nucleation from mass spectrometric observations of polymer intensity when large clusters are known to exist in the flow.

For $p_0 \gtrsim 4000$ torr an attempt has been made to estimate the mean velocity of these two distinct sets of monomers. The results of these estimates are shown by the dashed lines in Fig. 5b. The two sets of monomers have velocities of approximately 500 and 580 m/sec.

The presence of slower-moving clusters has been observed in an earlier investigation (Ref. 1). In this study the mass spectrometer was deliberately misaligned so that a portion of the molecular beam impinged upon the mass spectrometer head. Some of the resulting debris was ionized and drawn into the mass spectrometer and resulted in a distorted velocity distribution of the type shown in Fig. 6 for $p_0 = 6000$ torr. From these observations it is evident that when condensation has occurred in the expansion, the resulting mean velocity distribution can be significantly affected by (1) electron impact and (2) beam impact with any portion of the mass spectrometer head.

4.3 EFFECT OF SOURCE DIAMETER, PRESSURE, AND TEMPERATURE ON MEAN GAS VELOCITY

In the present discussion only those data obtained with the 20°K pumping skimmer and collimator will be considered. Gas velocity measurements have been obtained with a 295°K conical skimmer. However, these measurements are not considered in the present discussion since it has been shown (Ref. 10) that, when there is significant condensation, skimmers of this type can affect the measured mean velocity. Examples of experimental data obtained in the present investigation are presented in Fig. 7.

The data for argon and carbon dioxide are characterized by a pressure range where the velocity is essentially constant followed by a range where the velocity increases with increasing source pressure (Fig. 7). For argon, the limiting thermal velocity (i. e., $\sqrt{2 C_p T_0}$) has been calculated on the basis of measured source temperature and is found to be in fair agreement (approximately 4 percent) with the observed constant

velocity level. For carbon dioxide the calculated limiting thermal velocity is considerably larger than the observed constant velocity level (Fig. 7b). In the free-jet expansion of polyatomic gases of the type under investigation in the present study the expansion is so rapid that there is insufficient time for rotational and vibrational equilibrium to be achieved. The difference between the measured limiting velocity (Fig. 7b) and the theoretical limiting velocity is an indicator of the fraction of the total enthalpy locked into these internal degrees of freedom. For a given gas the source pressures at which the monomer and total beam velocity increase are the same (c.f., Figs. 7a and b). As has been stated earlier, the source pressure at which the velocity starts to increase has been assumed to be indicative of the early stages of condensation. The results of the present investigation for monomer and total beam velocities are summarized in Fig. 8.

The argon, nitrogen, and oxygen measurements cover a wide range of temperatures for a source diameter of 0.0386 cm (Fig. 8). These three gases indicate that the pressure at which the velocity increases varies as $T_o^{2.5}$. This variation with temperature also appears to satisfy the more limited data for the other gases and orifice sizes. These data (Fig. 8) have been replotted as a function of orifice diameter for a source temperature of 300°K (Fig. 9). The variation of critical source pressure with orifice diameter is a function of the gas under investigation. On the basis of the available data it is reasonable to suggest that these variations with source temperature, diameter, and gas provide a reasonable means of determining whether there is a significant degree of condensation in a free-jet expansion.

4.4 ESTIMATES OF MASS FRACTION OF CONDENSATE FROM GAS VELOCITY MEASUREMENTS

The energy equation for steady-state, one-dimensional flow with no condensation is

$$h_o = h_\infty + [(V_\infty)_{nc}]^2/2 \quad (1)$$

When there is condensation in the flow, the energy equation can be written (see Ref. 9) as

$$h_o + gL = h_\infty + [(V_\infty)_c]^2/2 \quad (2)$$

On combining equations (1) and (2) one can see that the increase in gas kinetic energy resulting from the addition of the latent heat of vaporization of the gas to the flow can be derived from

$$[(v_{\infty})_c]^2 - [(v_{\infty})_{nc}]^2 = 2gL \quad (3)$$

Values of $[(v_{\infty})_c]^2 - [(v_{\infty})_{nc}]^2$ for complete condensation of the gas are tabulated in Table I, Appendix II, for various gases and source temperatures. Also shown in Table I are the experimental values of $[(v_{\infty})_c]^2 - [(v_{\infty})_{nc}]^2$ for source pressures of approximately 10 atm. The ratio of the experimental to the theoretical maximum value yields the mass fraction of condensate, which is also tabulated in Table I. These values of mass fraction of condensate range approximately from 20 to 30 percent. It is of interest to note that for the 85°K nitrogen expansion (c.f., Fig. 5b) at source pressures greater than 4000 torr the condensed particles were large enough to be visible. This visual observation of condensed particles is consistent with the significant mass fraction (i. e., $g \approx 30$ percent) of condensate estimated from the velocity measurements.

In the commercial process to liquefy gases, the gas is expanded from high pressure, and fractions of condensate of approximately 25 percent are obtained (Ref. 11). The mass fraction of condensate estimated from the gas velocity measurements is consistent with these values.

4.5 ACCELERATION OF CLUSTERS IN FREE-JET EXPANSIONS

It has been indicated that after the onset of condensation the velocity of the noncondensed molecules is increased as a result of the release of the latent heat of vaporization. When this occurs, it seems reasonable to assume that the gas can be considered to be a binary mixture comprised of (1) large, slow-moving clusters and (2) fast monomers.

There have been many studies of the characteristics of free-jet expansions of gas mixtures. It has been assumed (Ref. 12) that if in the expansion of a gas mixture there are sufficient collisions to equilibrate the velocities between the two species, the heavy and light gas molecules will have the same velocity. Thus, if a dilute mixture of a heavy species in a light carrier gas is expanded, the lighter gas will in effect accelerate the heavier gas. For example, it has been found (Ref. 12) that the velocity of argon molecules in a beam generated from an argon-hydrogen mixture was on the order of the mean gas velocity. Further-

more, it was observed that argon concentration on the centerline was higher than the theoretical value, indicating an apparent enrichment of the heavy species.

It is suggested that the present studies of monomer/cluster mixtures are analogous, in some respects, to the above-mentioned studies of mixed-gas expansions. It has been suggested that the monomer velocity distribution characteristics of an 85°K nitrogen expansion (Fig. 6) indicate the presence of two distinct (fast and slow) groups of monomers. It has been postulated that the slow monomers result from fragmentation of the large clusters in the ionization region of the mass spectrometer. If this assumption is correct, then it is evident that the large clusters are not accelerated to the speed attained by the non-condensed monomers. This is not an unexpected result if it is accepted that the mass fraction of the condensate is on the order of 30 percent and the mean cluster size is in excess of 10^4 molecules. Equalization of the velocity of the light and heavy gas species has been achieved in mixed-gas expansions when concentration of the heavy specie in the mixture is small (i. e., less than 10 percent - Ref. 12) and the ratio of masses of the heavy to the light species is less than 20.

Some velocity measurements for a condensed carbon dioxide beam are shown in Fig. 10. On the basis of the above discussion for the 85°K nitrogen expansion it is assumed that the reduction in mean gas velocity at high source pressures results from significant contribution to the total signal from the large molecular clusters. It is of interest to note that at high source pressures the absolute level of the mean gas velocity is a function of the source skimmer separation distance (i. e., as this distance increases, so does the mean gas velocity).

In homogeneous condensation, cluster growth occurs as a result of molecular collisions and the resultant energy transfer between the condensing vapor and the noncondensed gas. Studies of free-jet expansions have demonstrated that a collisional freezing surface exists downstream of the source orifice (Ref. 12). The nature of the condensation process is such that it requires molecular collisions; therefore, no further cluster growth can occur when collisions cease (i. e., downstream of the collisional freezing surface). Downstream of the collisional freezing surface the pressure in the expansion continues to decrease until it falls below the vapor pressure of the clusters. When this occurs, the clusters will evaporate (or sublime), and the evaporated monomers will be introduced randomly into the flow at a higher energy than those remaining in the cluster. Given a sufficient flight distance (or time), it is

conceivable that the clusters will completely evaporate. In a molecular beam system the flight distance of the clusters is determined by the distance between the source and the detector. For the carbon dioxide velocity data shown in Fig. 10 the larger source-to-skimmer distance also means a larger source-to-detector distance. It is suggested that the difference in mean gas velocity for the condensed CO₂ beam may result from differences in the degree of evaporation of the clusters as a result of the differences in source-to-skimmer (detector) separation distances.

SECTION V CONCLUSIONS

When a gas condenses in a free-jet expansion, the latent heat of vaporization becomes available to heat the gas and thus to increase the translational velocity. At a fixed source-gas temperature a source pressure is reached where the velocity of the expanding gas starts to increase. It has been shown that the pressure at which this velocity increase occurs is related to the early stages of condensation in the expansion (i. e., the development of clusters of between 20 and 100 molecules). The source conditions at which this stage of condensation occurs have been determined for $85 \lesssim T_0 \lesssim 450^\circ\text{K}$ and $0.0147 \lesssim d \lesssim 0.1245$ cm for argon, oxygen, nitrogen, carbon monoxide, and carbon dioxide.

Estimates of the fraction of the gas condensed have been derived from the observed increase in gas velocity. These estimates show that for the source conditions of the present investigation the mass fraction of the condensate was approximately 20 to 30 percent.

Some velocity measurements obtained at two different source-to-skimmer separation distances are indicative of a contribution from evaporated or sublimated monomers. This is a problem of some interest in the sampling of condensed beams, and additional measurements would be of interest to determine the degree of evaporation that occurs.

REFERENCES

1. Bailey, A. B., Busby, M. R., and Dawbarn, R. "Cluster Formation in Free-Jet Expansions." AEDC-TR-72-32 (AD740898), April 1972.
2. Heald, J. H., Jr. "Performance of a Mass Spectrometric Modulated Beam Detector for Gas-Surface Interaction Measurements." AEDC-TR-67-35 (AD648984), March 1967.
3. Powell, H. M. and Heald, J. H., Jr. "A System for the Measurement of Velocity Distributions of Molecular Beams." AEDC-TR-68-151 (AD675306), September 1968.
4. Ruby, E. C., Brown, R. F., and Busby, M. R. "The Effects of Condensation on the Flow Field Properties in Free-Jet Expansions of Argon." AEDC-TR-70-142 (AD710616), August 1970.
5. Audit, Philippe. "Liasons Intermoléculaires dans les Jets Supersoniques Etude par Diffraction d'Electrons." Le Journal de Physique, Tome 30 (Fevrier-Mars 1969), pp. 192-202.
6. Hagena, O. F., Obert, W., and Wedel, H. V. "Condensation in Supersonic Free Jets: Experiments with Different Gases and Nozzle Geometries." Euromech 13 Meeting on the Aerodynamics of Rarefied Gas Flows. National Physical Laboratory, Teddington, Middlesex, England, July 1969.
7. Farges, J., Raoult, B., and Torchet, G. "Some Investigations of Molecular and Cluster Beams by Electron Diffraction: Structure, Size, Temperature." Eighth International Symposium on Rarefied Gas Dynamics, Stanford University, July 10-14, 1972. Abstracts, Vol. I, pp. 99-104, AFOSR-72-1276.
8. Gspann, J. "Cluster Sizes of Condensed Molecular Beams: Potassium Scattering Results Compared with Time-of-Flight Mass Spectrometry." Entropie, No. 42 (Nov.-Dec. 1971), pp. 129-132.
9. Sherman, P. M. "Condensation Augmented Velocity of a Supersonic Stream." AIAA Journal, Vol. 9, No. 8 (August 1971), pp. 1628-1630.

10. Bailey, A. B., Busby, M. R., and Dawbarn, R. "Effect of Skimmer Interaction on the Properties of Partially Condensed Molecular Beams." AEDC-TR-72-100 (AD746292), August 1972.
11. Lyon, D. N. "Production of Low Temperatures." Cryogenic Technology, Robert W. Vance, Editor. John Wiley & Sons, Inc., New York, 1963, pp. 9-59.
12. Abuaf, Nesim. "Molecular Beams from Free Jets of Pure and Mixed Gases." Princeton University, Ph. D., 1967. University Microfilms, Inc., Ann Arbor, Michigan (Order No. 67-9589).

APPENDIXES
I. ILLUSTRATIONS
II. TABLE

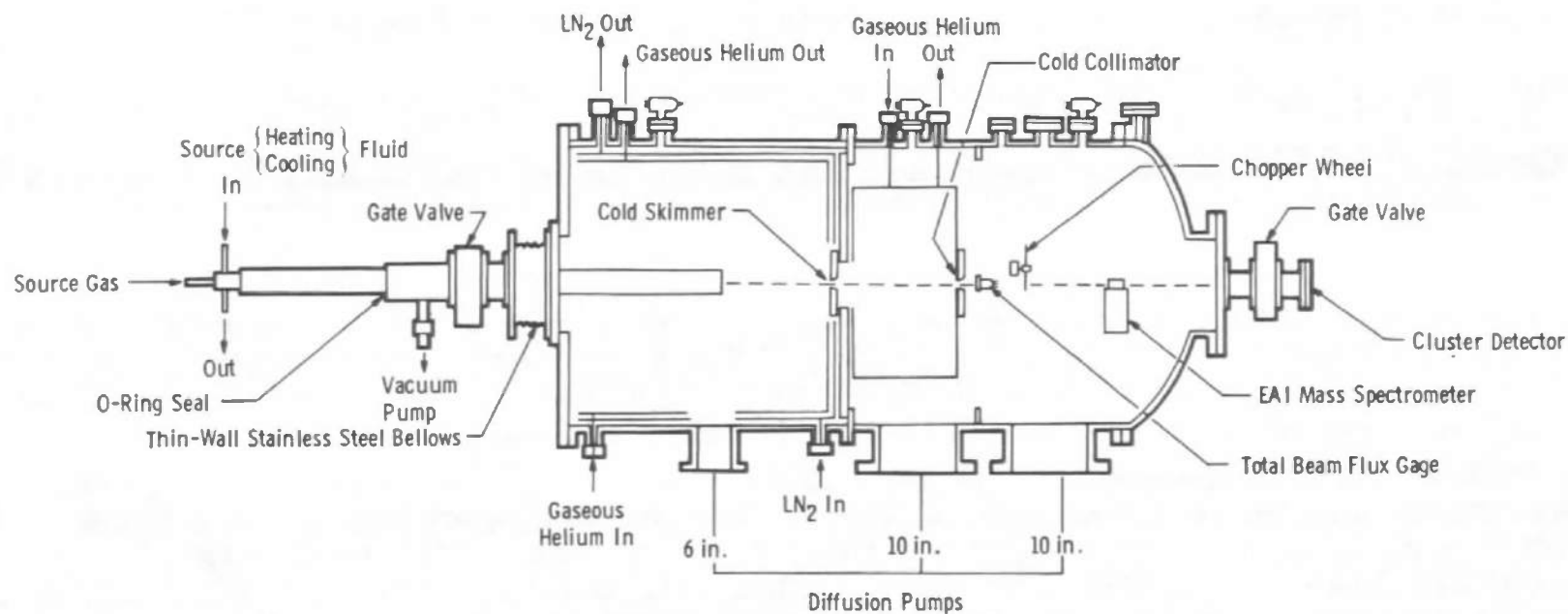


Fig. 1 Schematic of the Aerodynamic Molecular Beam Chamber

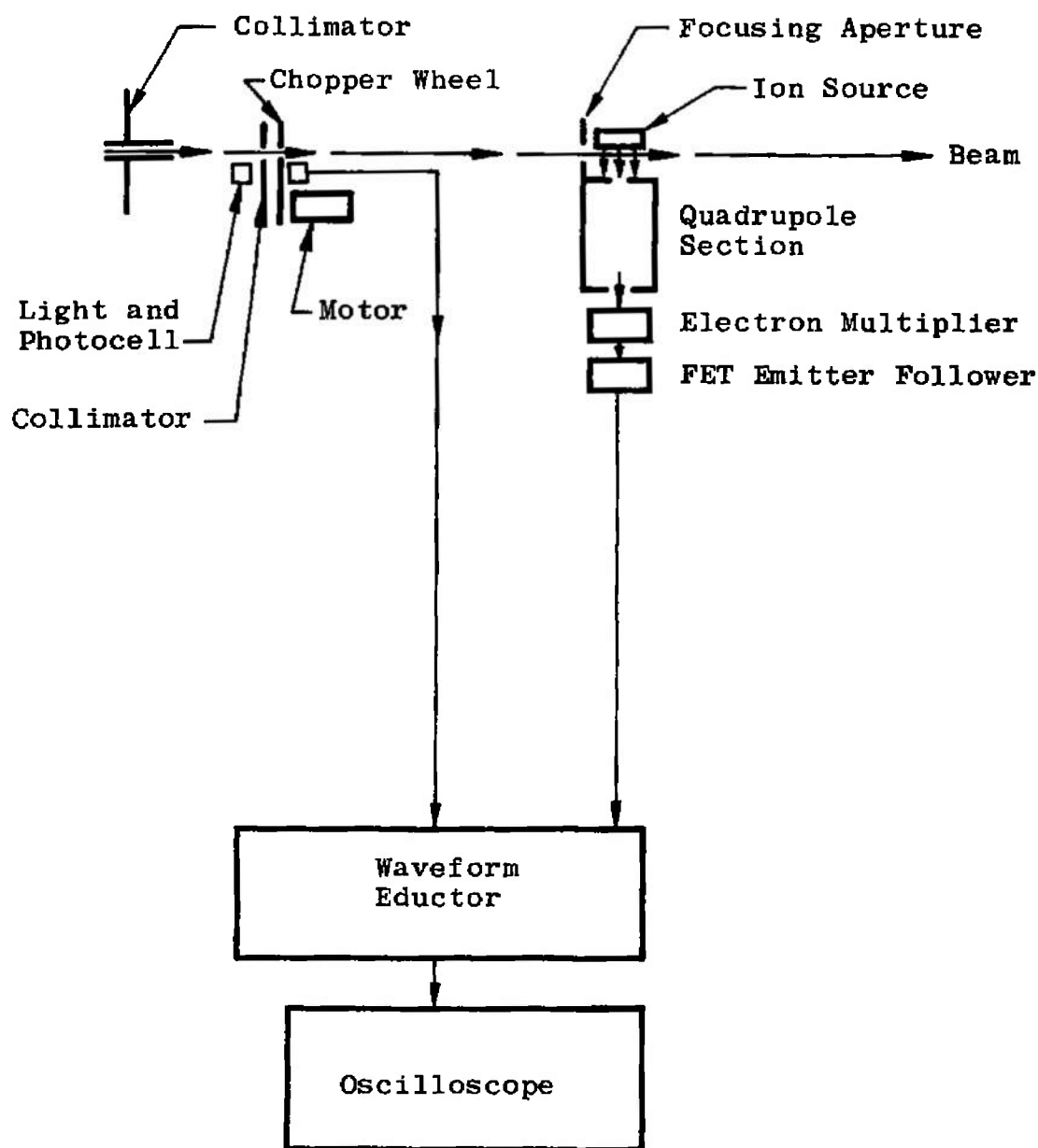
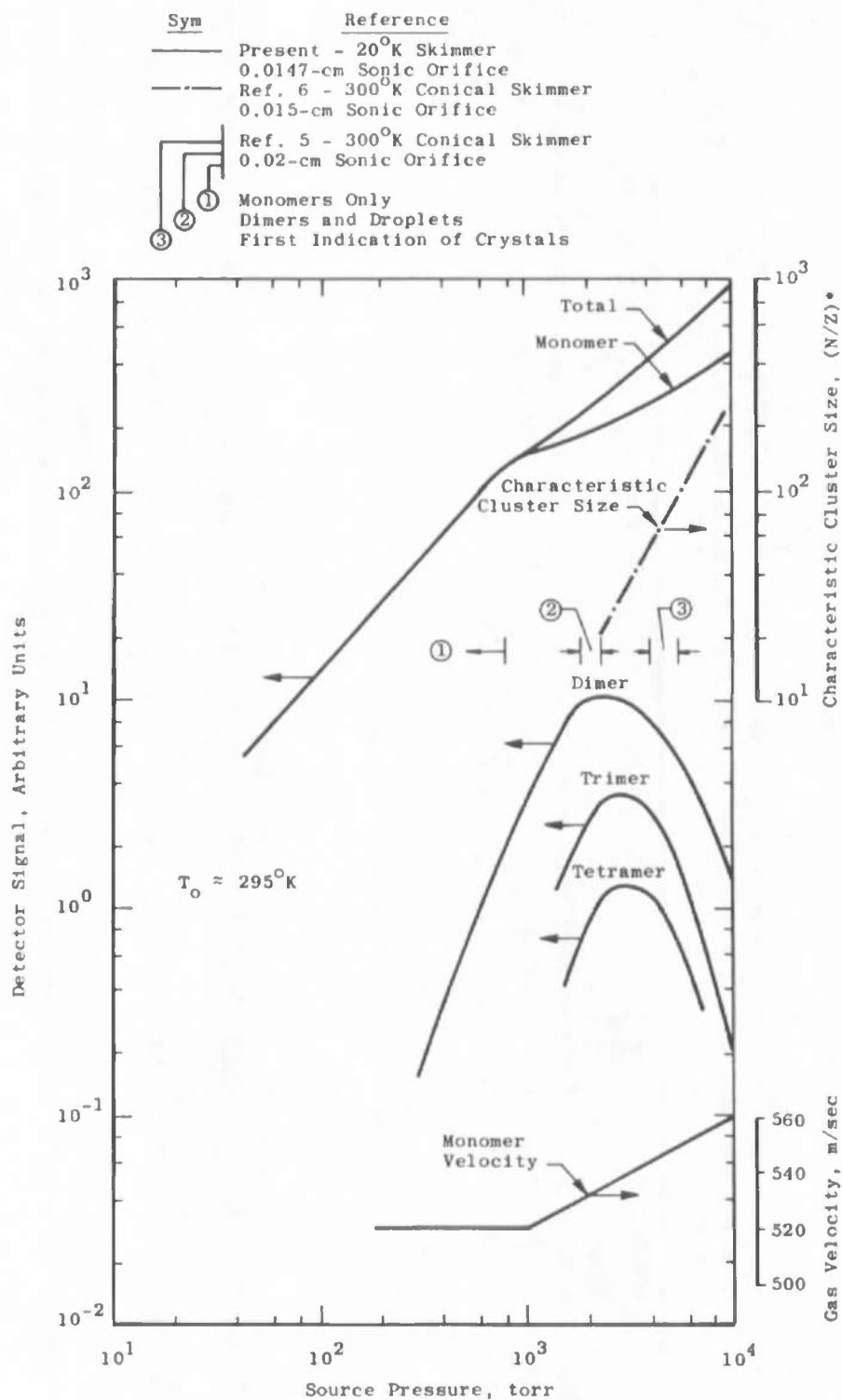
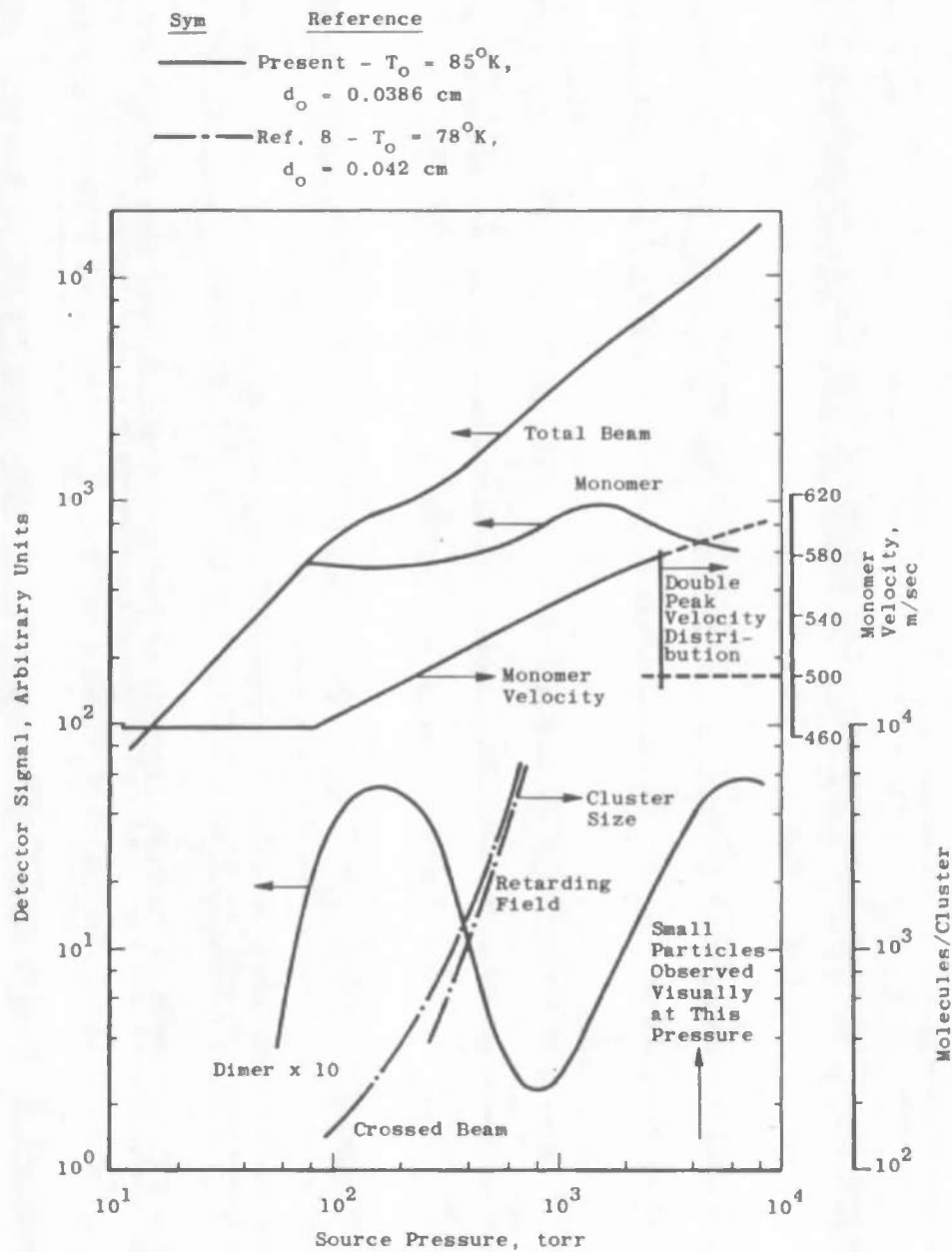


Fig. 4 Schematic Diagram of the Modulated Beam Detection System Used in the Time-of-Flight Measurements



a. Argon

Fig. 5 Indicators of Condensation in Free-Jet Expansions



b. Nitrogen
Fig. 5 Concluded

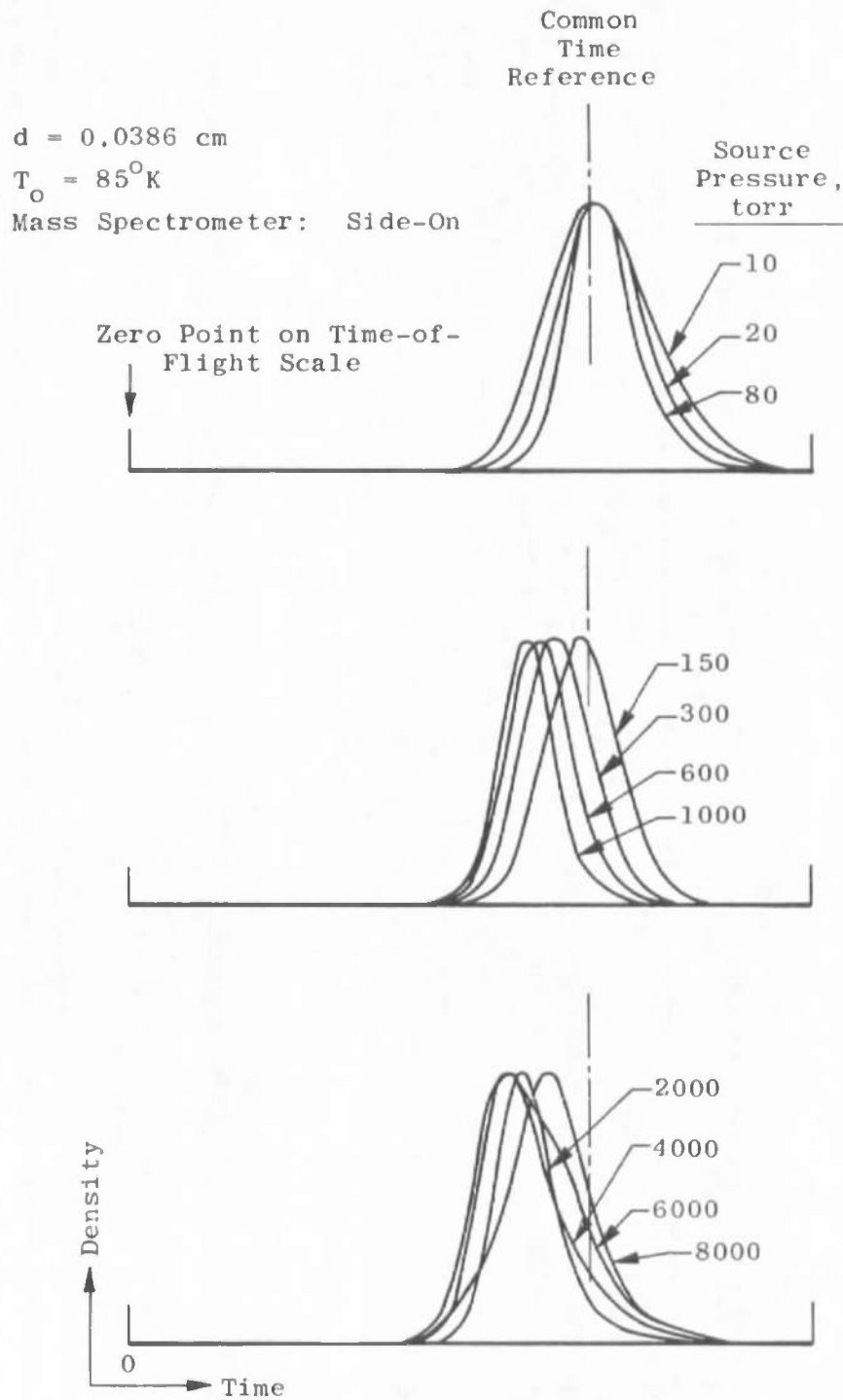
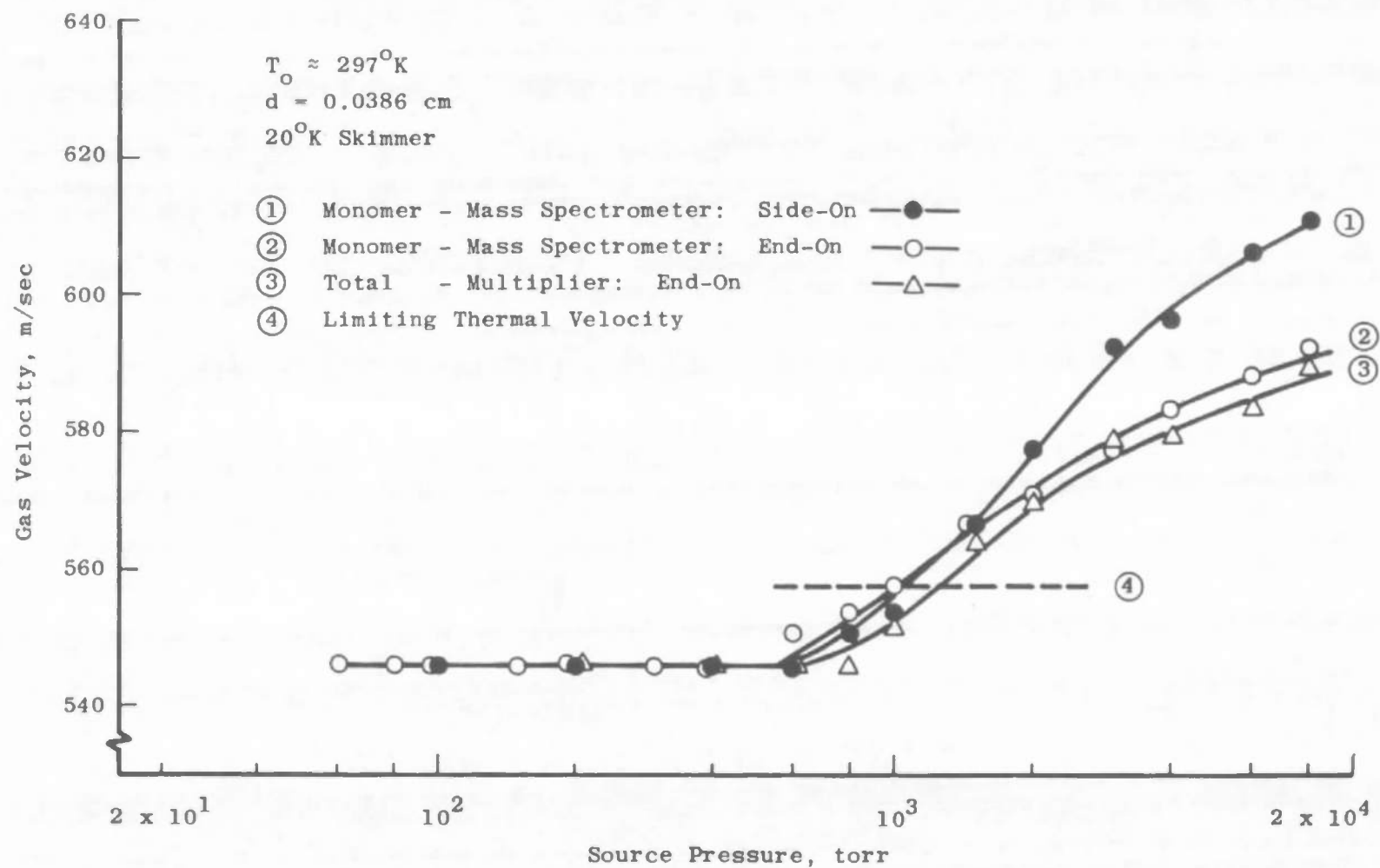
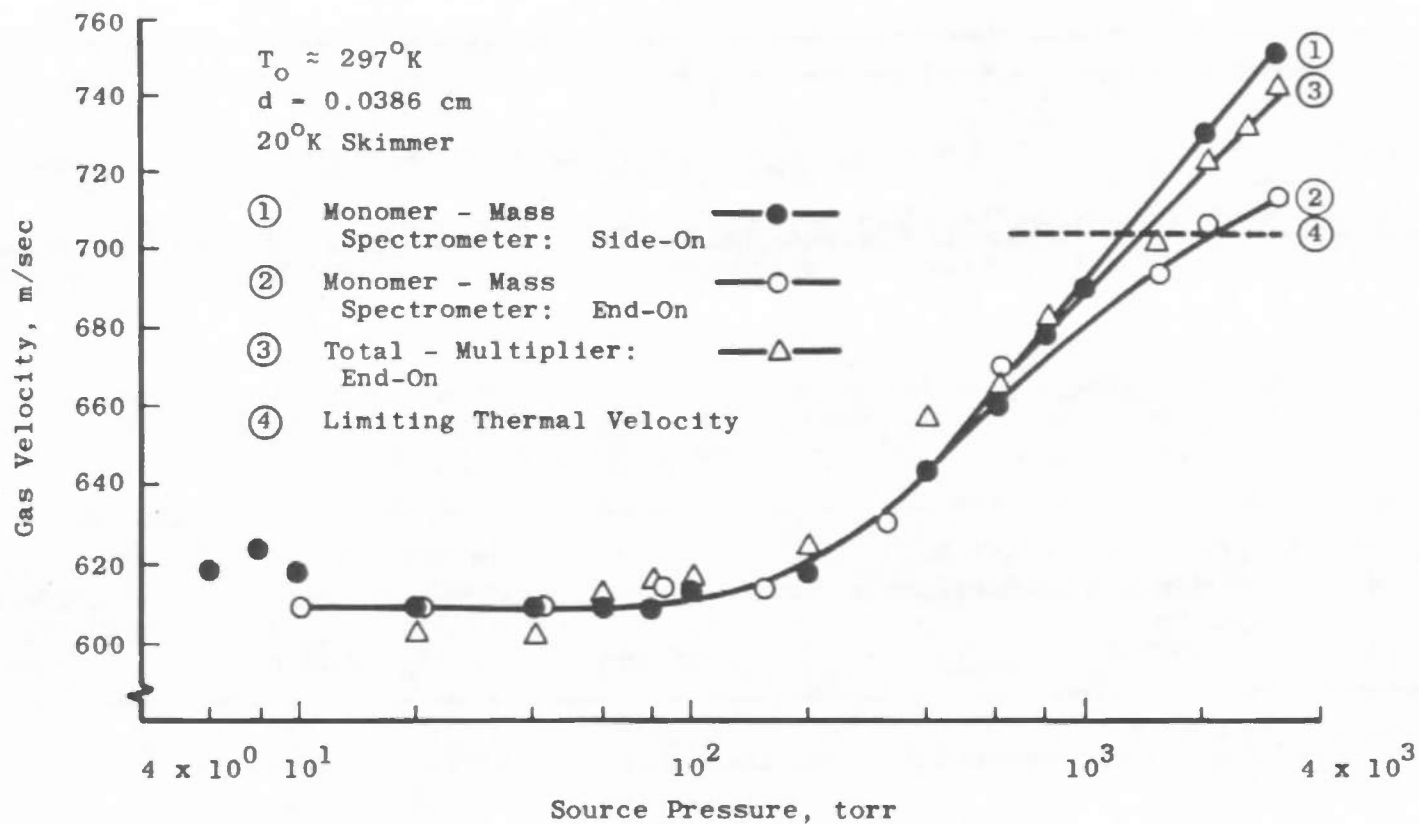


Fig. 6 Effect of Source Pressure on Monomer Velocity Distribution for Nitrogen



a. Argon

Fig. 7 Mean Beam Velocity as a Function of Source Pressure



b. Carbon Dioxide
Fig. 7 Concluded

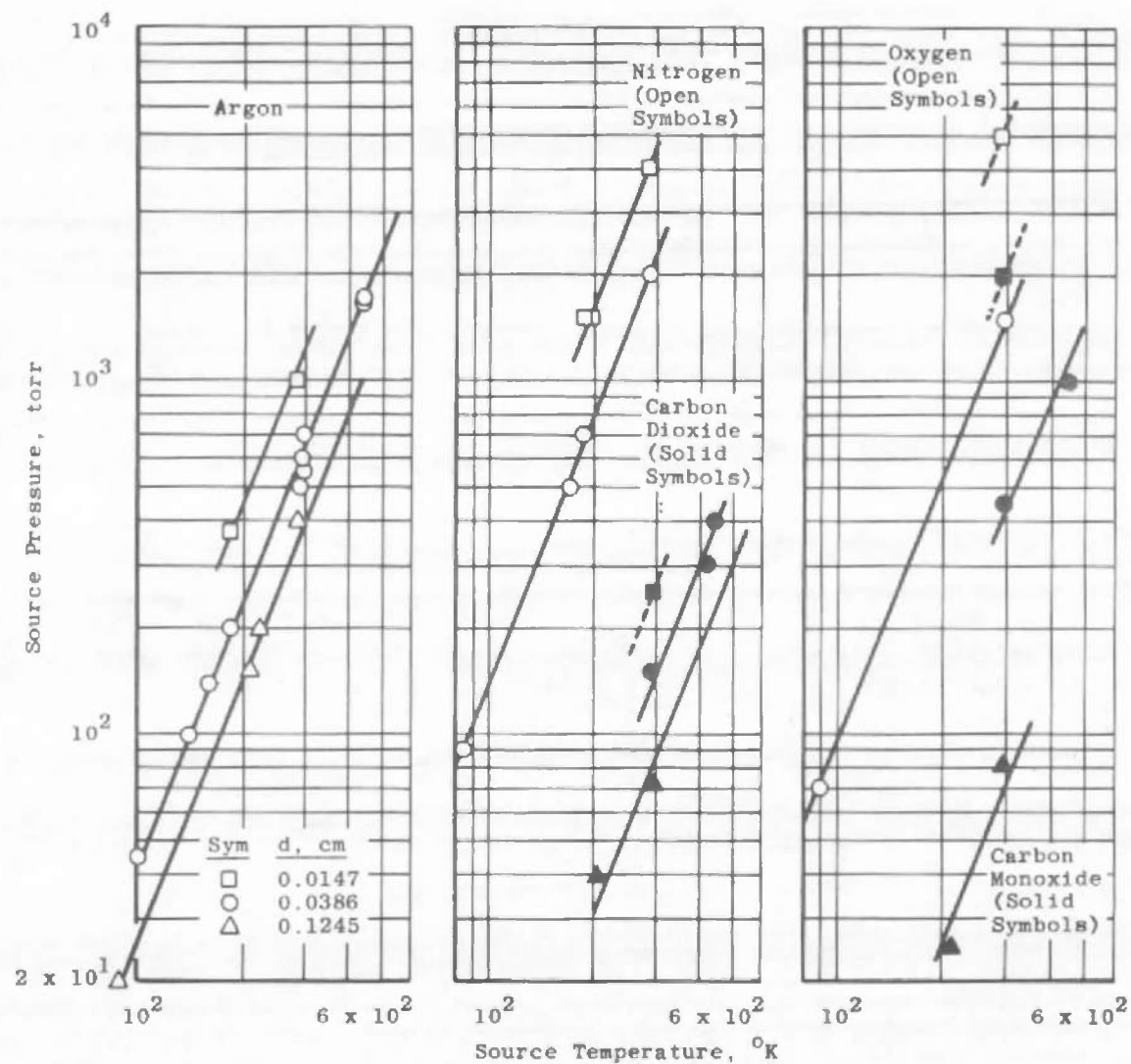


Fig. 8 Source Pressure at Which Gas Velocity Increases as a Function of Source Temperature

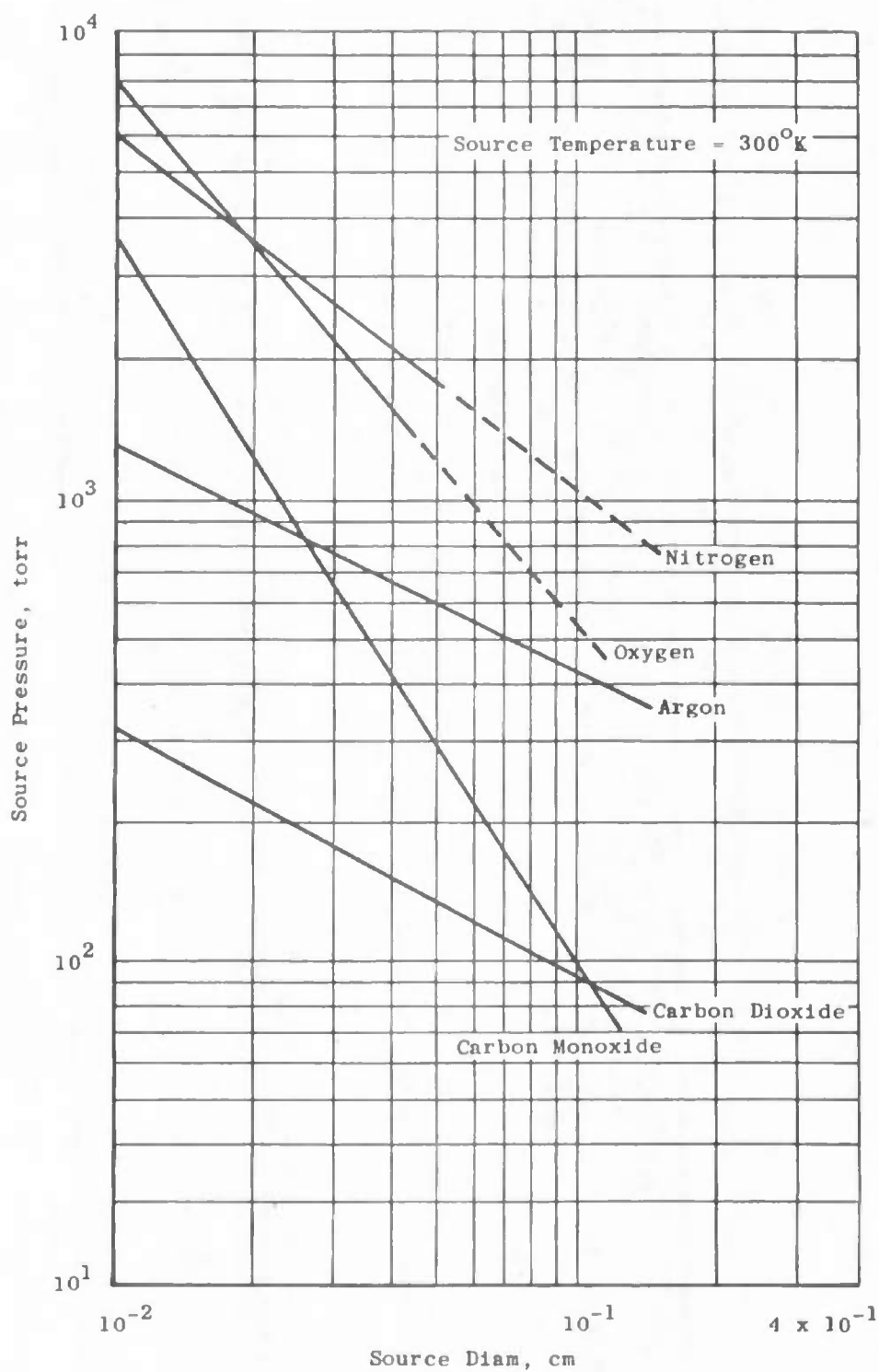


Fig. 9 Source Pressure at Which Gas Velocity Increases as a Function of Source Diameter

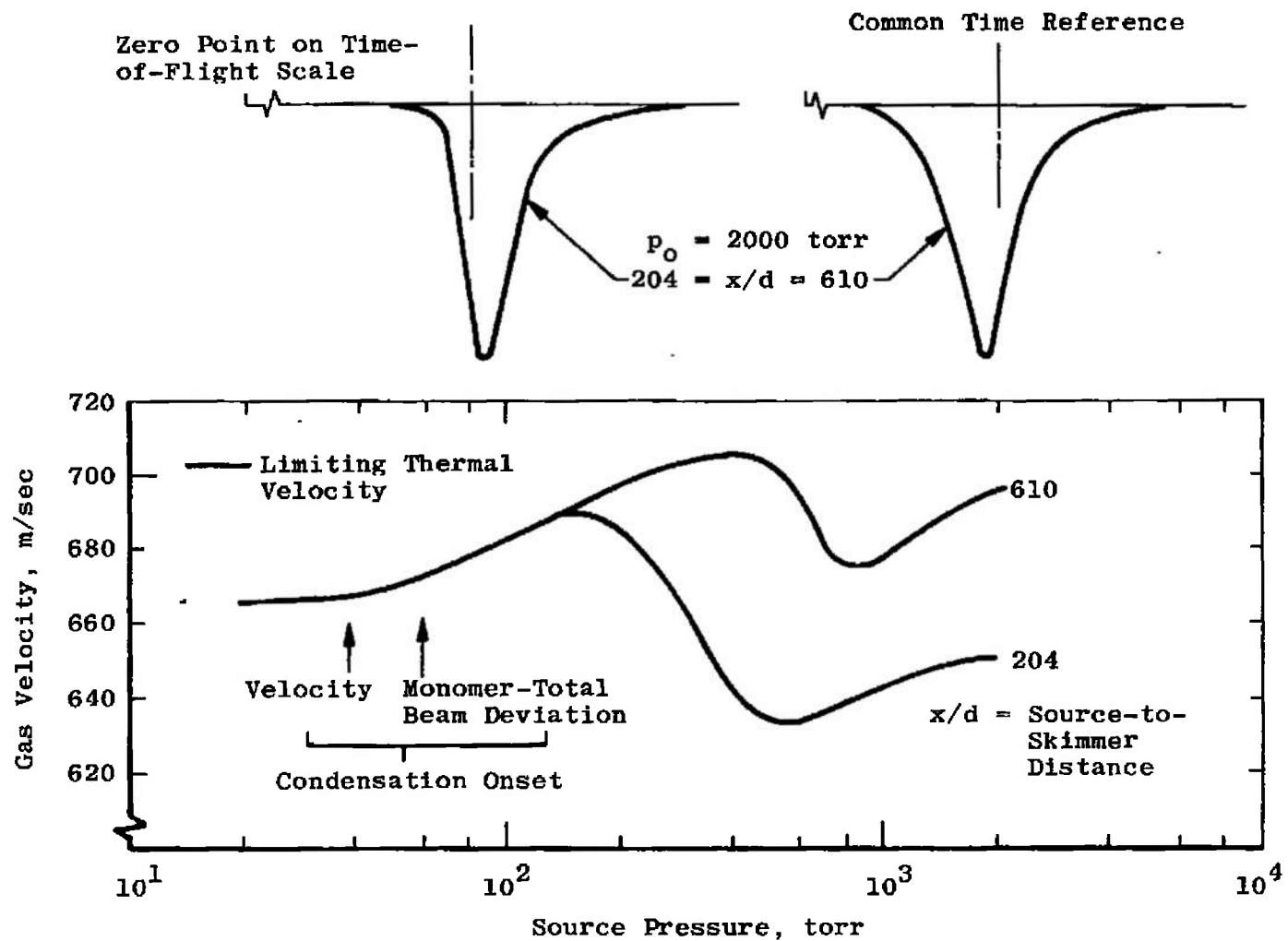


Fig. 10 Effect of Source-to-Skimmer Distance on Measured Total Beam Velocity in Condensed Flow of Carbon Dioxide

TABLE I
MASS FRACTION OF CONDENSATE DERIVED
FROM MEASUREMENTS OF BEAM VELOCITY

Orifice Diameter = 0.0386 cm					
Source Stagnation Pressure \approx 10 atm.					
	Argon	Nitrogen	Oxygen	Carbon Dioxide	Carbon Monoxide
Latent heat of Vaporization, cal/gm	37.6	47.6	50.9	87.2	50.4
$(V_{\infty})_c^2 - (V_{\infty})_{nc}^2$ for $g = 100$ percent, $m^2/sec^2 \times 10^{-4}$	31.5	39.8	42.6	73.0	42.2
Source Stagnation Tempera- ture, $^{\circ}K$	297	85	90	297	450
Experimental Values $(V_{\infty})_c^2 - (V_{\infty})_{nc}^2$, $m^2/sec^2 \times 10^{-4}$	8	12	8	20	11
Mass Fraction Condensate, percent	25	30	18	27	26

UNCLASSIFIED

Security Classification

14

KEY WORDS

LINK A

LINK B

LINK C

ROLE

WT

ROLE

WT

ROLE

WT

1 spectrometers

molecular beams

2 cryopumping

skimmers

condensation

velocity

vacuum chambers

argon

carbon dioxide

nitrogen

oxygen

carbon monoxide

3. Condensation

4. Gas velocities

Condensation

UNCLASSIFIED

Security Classification